The Analyses of Extended Shear Tab Steel Connections Part II: Stiffened Connections

MUSTAFA MAHAMID, ADEEB RAHMAN, and AL GHORBANPOOR

Modeling of extended shear tab connections has been investigated using computational nonlinear mechanics. While the details of the modeling and the analyses of unstiffened extended shear tabs have been addressed in Part I (Rahman, Mahamid, Amro, and Ghorbanpoor, 2007), this paper addresses in detail the analyses and failure prediction of the stiffened shear tab connection. Correlation between the results of the computational finite element method and the experimental investigation is established and verified. Past experimental investigations have shown that the unstiffened shear tab connections are prone to twisting failure and low load-carrying capacity. Therefore, the use of stiffened shear tab connections is a viable design approach to overcome these problems. Finite element analysis (FEA) of stiffened extended shear tab connections in the plastic range requires special treatment because of the inherent material nonlinearities and the nonlinear modeling required to prescribe contact surface. The various predicted failure modes from a finite element analysis are compared with those observed in a recent experimental study performed by Sherman and Ghorbanpoor (Sherman and Ghorbanpoor, 2002). The study documented new limit states including twisting of the shear tab and column web mechanism. Three-, five-, and eight-bolt stiffened extended shear tab connections were used in beams that were framed into supporting girders or columns. A new design methodology was introduced for these types of connections. In addition, five finite element (FE) models of two-bolt and deep connections are analyzed in the plastic range to predict their failure modes. These connection models are two-bolt beam-to-column, 10-bolt beam-to-girder, 10-bolt beam-to-column, 12-bolt beam-to-girder, and 12-bolt beam-to-column.

Mustafa Mahamid is a structural engineer, Graef, Anhalt, Schloemer, and Associates, Milwaukee, WI.

Adeeb Rahman is associate professor, department of civil engineering and mechanics, college of engineering and applied science, University of Wisconsin–Milwaukee, Milwaukee, WI.

Al Ghorbanpoor is professor, department of civil engineering and mechanics, college of engineering and applied science, University of Wisconsin–Milwaukee, Milwaukee, WI.

LITERATURE REVIEW

Astaneh, Call, and McMullin (1989) and Richard, Gillett, Kriegh, and Lewis (1980) have performed research on standard shear tab connections and a design procedure has been developed from each study. Their studies investigated the shear tabs when welded to the flange of wide-flange columns. The failure modes outlined by their studies are: shear failure of bolts, yield of gross area of plate, fracture of net area of plate, fracture of welds, and bearing failure of the beam web or plate.

Chiew, Lie, and Dai (2001) analyzed the moment resistance of steel I-beams connected to concrete filled tubes (CFT) using the commercial finite element software MARC. Eight connections were investigated and tested to failure; four specimens were semi-rigid beam-to-column connections and four specimens were rigid connections. The research focused on the study of the capacity of the connection and its moment resistance at the yielding state, which was compared to an empirical formula. The proposed formula by Chiew et al. (2001) was effective in predicting the moment resistance of the connections.

Butterworth (2003) presented a finite element analysis to investigate extended end-plate beam-to-column connections. Experiments were done for an extended end-plate connection that consisted of a plate welded to the end of the steel beam. The FEA analysis, using MYSTRO and LUSAS FE software, implemented strain solids and contact gap elements to model the connection behavior. The Green Book design method developed by the Steel Construction Institute (SCI) and the British Constructional Steel Work Association (BCSA) requires increased connection capacity. Butterworth's work is designed to investigate this recommendation. In both the FEA and laboratory tests, it was found that the Green Book design theory consistently underestimated the bolt forces in the top rows of the connection and overestimated the forces in the lower rows. The experimental and FEA results were in the same range of accuracy; 80% in most of the cases.

Sherbourne and Bahaari (1994) developed a 3D finite element model to evaluate the moment rotation relationship for steel bolted end-plate connections. They performed a 3D analysis using ANSYS finite element software. The investigators concluded that the average behavior of the end-plate connections, up to the ultimate load, was successfully simulated through the three-dimensional model by using plate, brick, and truss elements. The model showed lower stiffness than the test results, but it was within a 75% range of accuracy.

Bursi and Jaspart (1994) performed numerical analysis of steel bolted extended end-plate moment resisting connections using finite element models in both elastic and plastic ranges. A three-dimensional nonlinear finite element model suitable for the analysis of extended end-plate connections was proposed and validated. The FEA results were compared to the experimental results and showed 80% agreement in most of the investigated cases. In a related study Bursi and Jaspart (1997) presented finite element analysis of two-bolt T-stub connections. The purpose of their study was first, to validate the finite element software package LAGAMINE, and second, to establish a rational approach to calibrate the finite element model to be able to produce elastic-plastic behavior. Results were compared to experimental data from tests conducted by the investigators. The T-stub connections failed in different plastic failure mechanisms, which were adopted as benchmarks in the validation process of the finite element package.

Yang, Murray, and Plaut (2000) investigated the tension and shear behavior of double angle connections using ABAQUS. The connections were subjected to axial tensile loading, shear loading, and combination loading. The study reported that the thickness of the connection angle has a significant influence on the response of the connection in shear and in tension loading. The complex connection behavior stems from part separation, bolt slip, bolt pretensioning, and inelastic behavior.

Sherbourne and Bahaari (1996) proposed a 3D finite element model to study the behavior of the bolted T-stub to unstiffened column flange connections. ANSYS finite element software was used in the analysis. It was observed that prying forces on the T-stub increase with a decrease in the relative stiffness. It was observed also that the material properties of the flanges were important for predicting the behavior and force distribution of T-stub connections. There was a good correlation between the finite element and the test results. The same behavior in prying action was obtained in both the test and the finite element model. The range of agreement was 85%.

Gebbeken, Rothert, and Binder (1994) investigated the finite element modeling of bolted extended end-plate steel connections to predict their behavior and load-carrying capacity. It was observed that the connection element's contact effect and the material's hardening/softening effects had to be considered to achieve accurate analysis. It was also found that an accurate connection behavior in the plastic range could be predicted only when three-dimensional brick elements were used in the analysis.

The literature review and the experimental study performed by Sherman and Ghorbanpoor (2002) strongly suggest the necessity to study the behavior of the stiffened extended shear tab connections in a computational model and to expand the experimental study to shallower and deeper connections. The commercial code ANSYS version 7.0 has excellent capabilities to model these types of connections that were not available in other commercial codes used to model steel connections, as mentioned earlier.

Prior to extending the limit of application to connections beyond those examined in the experimental study, FE models were developed to simulate the framing members and connections of the experimental work. The experimental results from the study by Sherman and Ghorbanpoor (2002) provided the basis for optimizing the parameters utilized in the FE models.

3D FINITE ELEMENT MODELING

A 3D FE model is constructed to represent the geometry of the shear tab connection and the associated structural details. As presented by Rahman et al. (2007), four finite element types are used in the modeling of beams, columns, shear tabs, and bolts. These elements are:

1. 3D brick elements to model the beam, supporting members, and the shear tab.

2. 3D tetrahedral elements to model the bolts where the elements have curved edges appropriate for the bolt geometry.

3. Pretensioning elements to model the pretensioning force in the bolts.

4. Contact elements to create contact surfaces to transfer the forces from the beam to the shear tab and on to the bolts.

Friction plays a main role in transferring forces between surfaces (Rahman et al., 2007). Contact elements can accurately account for friction. In this structure, the beam web is in contact with the shear tab as shown in Figure 1. Contact is also established between the beam web and the head of each bolt and between the shear tab and the nut of each bolt. There is also contact between the bolt shanks and the bolt holes in both the shear tab and the beam web. A surface-to-surface, flexible-to-flexible contact element type is used to simulate contacts between the steel surfaces (ANSYS, 2002). The flexible-to-flexible is used because the surfaces in contact are made from steel deformable material. Table 1 shows the structural members and the geometric properties of the extended shear tabs investigated in this study. The finite element models for the 10-bolt beam-to-girder connection and the 12-bolt beam-to-column connection are shown in Figures 2 and 3, respectively. Figure 4 shows the shear tab and the stiffeners for the 12-bolt beam-to-column connection.

Material Properties

Each shear tab in this study is ASTM A36, the bolts are ASTM A325-X, and the structural members are ASTM A572 Grade 50 steel. The following parameters are used in the FE analysis for this study: a coefficient of friction equal to 0.30 provided the best convergence in the FE analyses. Mechanical tests are performed to obtain the stress-strain response of the steel shear tabs, bolts, and the column web. With the three-bolt connection, a bilinear stress-strain response was defined in the FE model by specifying the experimental results of the yield strength, ultimate strength, tangent modulus which is based on the elongations, and the modulus of elasticity (see Table 2). In the FE model with the six-bolt and the eight-bolt connections, the experimental stress-strain responses are specified in Figure 5. The stress-strain response for the bolts is shown in Figure 6. The material properties used for the FE analysis of 10-bolt and 12-bolt connection models are the same as those used in the eight-bolt connection.

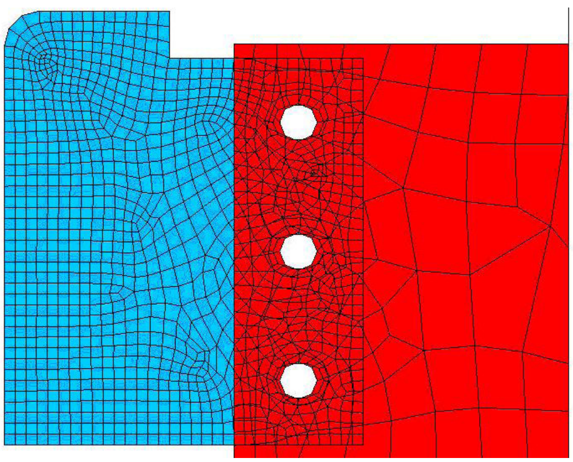

Fig. 1. Contact between the shear tab and the beam's web (three-bolt connection).

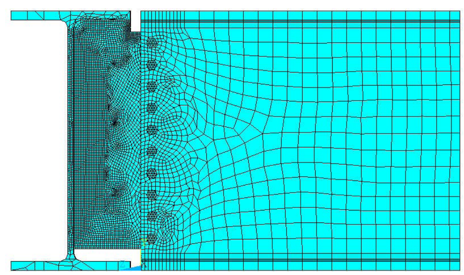

Fig. 2. Finite element model for the 10-bolt beam-to-girder connection.

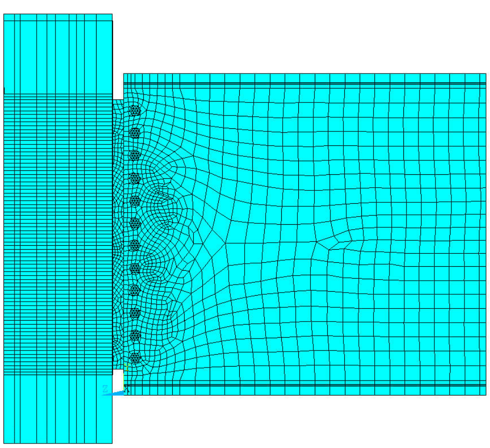

Fig. 3. Finite element model for the 12-bolt beam-to-column connection.

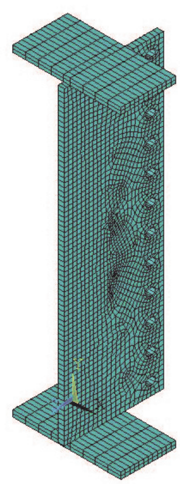

Fig. 4. Shear tab and stiffeners for the 12-bolt beam-to-column connection.

Table 1. Geometric Parameters and Yield Strength for Investigated Connections							
Connection	Beam	Supporting Member	Beam Length (ft)	Supporting Girder		Shear Tab	
				Length (ft)	Yield Strength (ksi)	Thickness (in.)	Yield Strength (ksi)
Three-bolt	W12×87	Girder = W14×53	30	10	55.5	0.25	45.7
Six-bolt	W24×146	Girder = W30×90	33	10	53.4	0.3125	46.3
Eight-bolt	W30×148	Column = W14×90	33	8	63.5	0.375	52
10-bolt beam-column	W36×230	Column = W14×90	39	8	63.5	0.5	52
10-bolt beam-girder	W36×230	Girder = W36×230	39	10	63.5	0.5	52
12-bolt beam-column	W44×230	Column = W14×90	46.5	8	63.5	0.5	52
12-bolt beam-girder	W44×231	Girder = W44×230	46.5	10	63.5	0.5	52
Two-bolt	W12×87	Column = W8×31	30	8	55.5	0.375	45.7

Table 2. Three-Bolt Model Material Properties			
Member	Yield Strength (ksi)	Ultimate Strength (ksi)	Elongation (%)
¼ in. shear tab	45.7	69.8	30
W14×53 web	55.5	73.8	29

RESULTS AND DISCUSSION

The results report the behavior of the extended shear tab connections generated by the FE analyses and are observed and recorded in the experimental investigation. The ultimate load-carrying capacity of the connection is measured in the experiments and calculated in the FEA for each connection. The behavior, reported as a function of the applied shear force at the connection, is outlined through following the

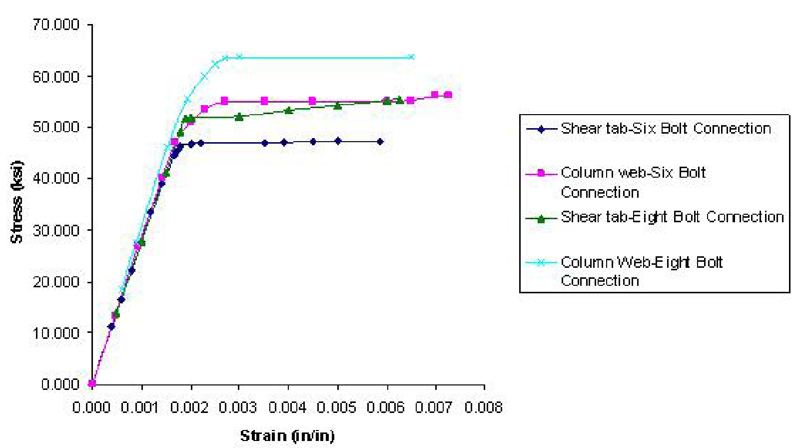

Fig. 5. Stress-strain curve for structural members and shear tabs.

connection's response: vertical displacement of the connection along the bolt line, shear load eccentricity relative to the connection bolt line, twisting of the connection plates, nonlinearity, and failure modes.

Vertical Displacement

The experimental study was limited to connections that included three, six, and eight bolts, as reported by Sherman and Ghorbanpoor (2002). In this FE study, finite element models were developed for those connections used in the experiment to establish the governing analytical parameters to achieve good accuracy in the results. Using the established FE parameters, additional FE analyses were performed to develop an understanding of the behavior of the shallow beam-to-column connection with two bolts and the deeper beam-to-column and beam-to-girder connections with 10 and 12 bolts.

Figure 7 shows the vertical displacement of the plate due to shear force for a connection with three, six, and eight bolts. The curve shows the experimental and the corresponding finite element readings. It is observed that good agreement exists between the experimental and the FE results. The figure also shows that as the number of bolts is increased, the connection response becomes closer to the behavior of rigid connections. The connection behaves as if it were connected to a rigid support.

Figure 8 shows the finite element results of the vertical displacement of the plate due to shear for deep connections of 10 and 12 bolts. The results in the figure are for beams being framed either to supporting girders or supporting columns. Figure 9 shows the shear versus displacement curve for the two-bolt connection generated from the FE analysis. The figures show the elastic and the plastic behavior of the connections up to failure.

Shear Load Eccentricity

Experimental and FEA eccentricity results at failure are presented in Table 3 for all the connections discussed in this paper. The eccentricity sign convention is shown in Figure 10. It is observed from Table 3 that the experimental and the FEA regression analysis eccentricity results are in good correlation with a deviation maximum of 13%. However, the eccentricity results from the location of the zero strain readings are slightly different because the linear regression analysis procedure is approximate but acceptable. It was also observed that the eccentricity values for the deep connections were close to eccentricity values obtained from AISC (1995, 1998) for the rigid connections. This shows that the behavior of the deep extended shear tab connections is similar to the behavior of the rigid connections.

Twisting of the Connection Plates

Twisting of the connection plates was more significant in the unstiffened connections as reported in Part I (Rahman et al., 2007). Twisting was also observed in the stiffened connections for the case of the beam framed into a girder and for deep connections when the beam is framed into a column. Twist was evident in the eight-bolt connection in both the experiment and the FEA results. In the experiment, buckling of

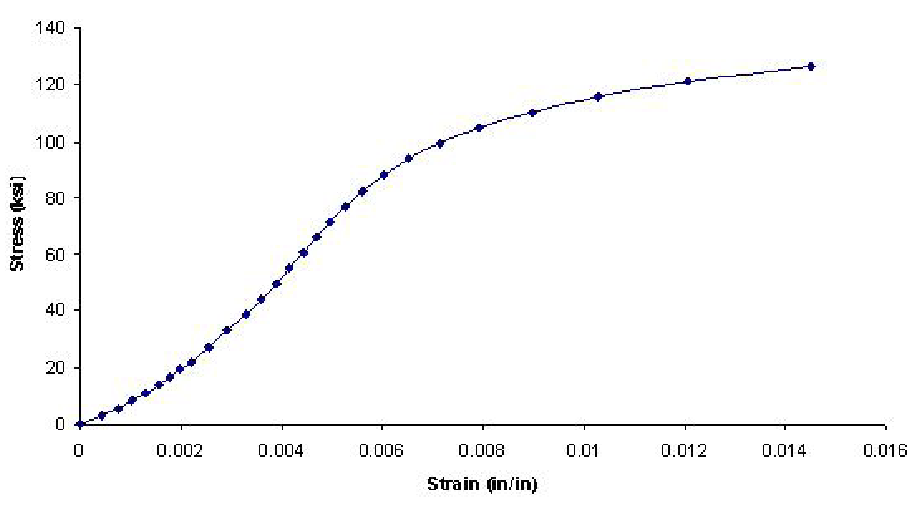

Fig. 6. Stress-strain curve for A325 bolts.

Table 3. Eccentricity Results					
Connection	Eccentricity (in.)			AISC Eccentricity (in.)	
	Experiment	FEA*	FEA**	Flexible	Rigid
Three-bolt	–2.09	–2.10	–2.25	6.50	4.50
Six-bolt	–4.89	–4.37	–3.20	8.96	4.96
Eight-bolt	–1.48	–1.67	–2.00	8.93	1.93
10-bolt beam-column	–	–1.74	–1.90	8.93	2.26
10-bolt beam-girder	–	–1.98	–1.50	9.82	3.15
12-bolt beam-column	–	–1.14	–1.10	8.83	0.83
12-bolt beam-girder model	–	–1.64	–1.00	9.64	1.64
Two-bolt model	–	–0.80	–0.30	5.91	4.58

*Regression analysis results.
**Location of zero strain at the top flange.

the shear tab was identified as a secondary failure mode due to the twist of the tab. Buckling analysis was not performed in the finite element model, but twisting was observed in the form of a second-mode shape of buckling.

In the connections where the beam is framed into girders, three-bolt, six-bolt, 10-bolt, and 12-bolt connections, twist was observed at the lower part of the shear tab. This behavior was observed in both the experiments and the FEA results and was expected due to the fact that the shear tab is stiffened at the top by the top flange of the girder and not stiffened at the bottom. A discussion of identifying twist as a failure mode for some of the investigated connections is presented later.

Nonlinearity

Nonlinearity is one of the most important aspects in the behavior of these connections. Its importance appears in identifying the failure modes of each connection. Experimentally, nonlinearity was studied by investigating the shear-displacement and shear-twist, and by observing the plastic

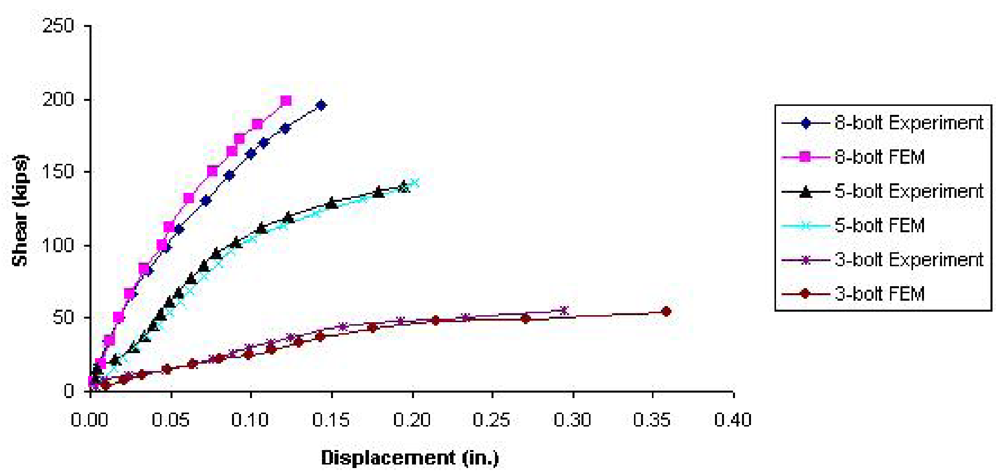

Fig. 7. Shear vs. displacement curves for three-, six-, and eight-bolt connections.

deformations at different locations in the shear tab and in the supporting members. As mentioned earlier, several parameters were studied to simulate the nonlinear behavior, such as contact elements, which make the model nonlinear once they are used in the model. In addition, the nonlinearity is present when defining the material properties of the structural components. Nonlinear behavior was studied in the FE models by analyzing the shear-displacement curves and by monitoring the stresses and plastic deformations at different locations in the connections. The tested and the analyzed connections were loaded to failure and exhibited a visible nonlinear behavior. The nonlinear behavior is observed in shear versus displacement curves as shown in Figures 7, 8, and 9.

Principal strains were monitored at the rosette strain gauge, which is located at $L/3$ from the shear tab's top edge and 1.5 in. from the side edge, where L is the depth of the shear tab. In the experimental work, the first principal strains

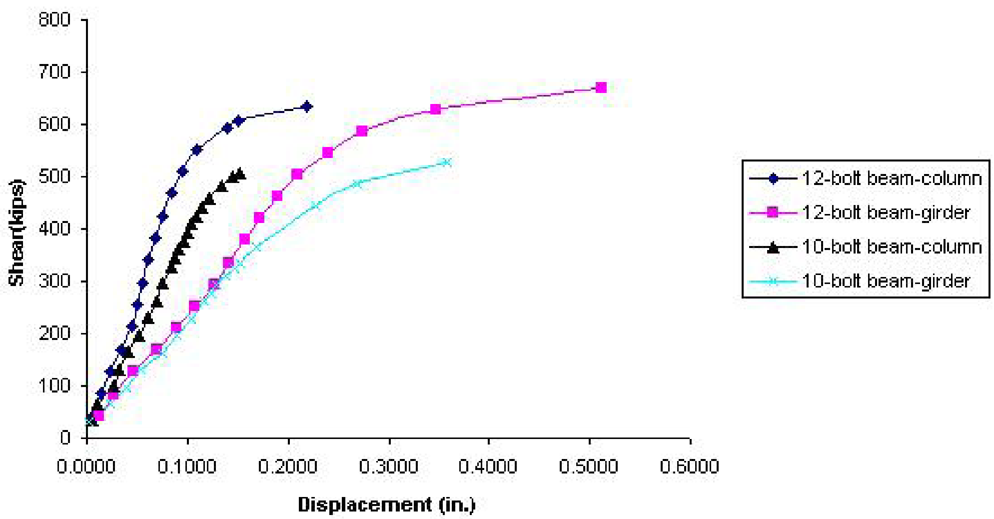

Fig. 8. Shear vs. displacement for the 10- and 12-bolt connections.

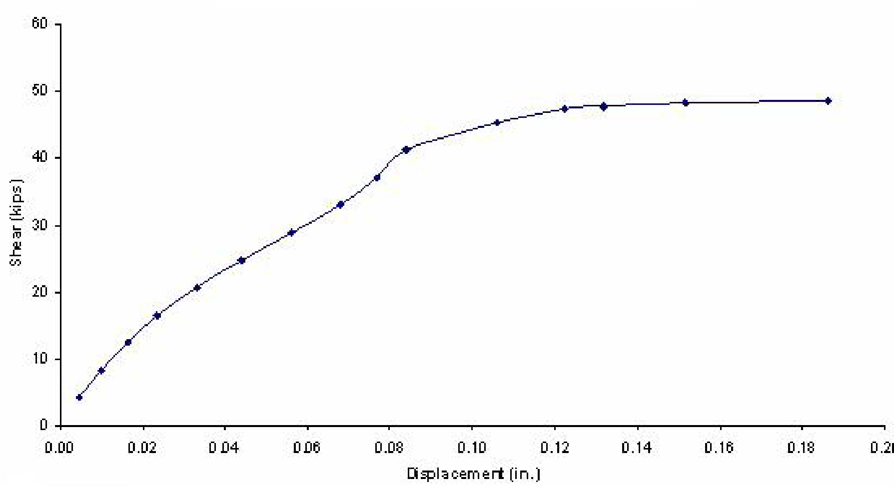

Fig. 9. Shear vs. displacement for the two-bolt connections.

were obtained from the measured strains using the three strain readings obtained from the rosette. In the FE analysis the first principal strains were measured directly at the same location. Figure 11 shows the shear versus principal strains for the three-, and six-bolt connections. The experimental results for the three-bolt connections are not available; however, the FE analysis results are provided. The FE results show that the shear tab has yielded. The figure shows good agreement between the experimental and the FE analysis results. Figure 12 shows the FE analysis results for the 10- and 12-bolt connections; the figure shows that the shear tab at that location has not yielded and has remained in the elastic range. This criterion is used to identify if the shear yield is a failure mode for these connections. The results show that shear yield is a failure mode in the three-, six-, and eight-bolt connections, and shear yield is not a failure mode for the 10- and 12-bolt connections.

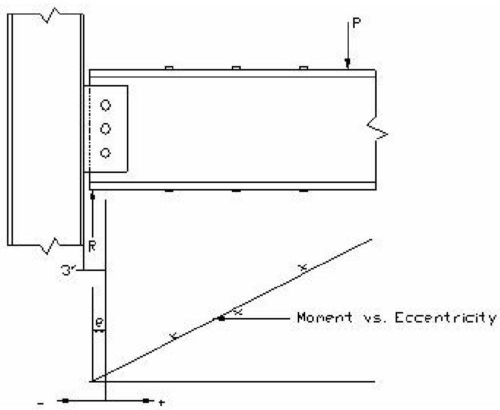

Fig. 10. Eccentricity sign convention.

High stresses and plastic deformation were also observed at bolts and at bolt holes in all the connections. This shows that the bolts and the bolt holes undergo nonlinear behavior and plasticity. The stresses that developed in the bolts and the bolt holes are shown in Figures 13 and 14. These stresses exceed the defined yield strength of the bolts and the shear tab. Plasticity was also observed in the supporting girders and at the lower tip of the shear tab. This is due to load transformation from the shear tab to the supporting girders. High stresses exceeding the defined yield stress are developed as shown in Figure 15.

Failure Modes

In testing the extended shear tab connections, the methodology followed by Sherman and Ghorbanpoor (2002) to identify the failure modes was to monitor the shear versus displacement curves, shear versus principal strain in the shear tab, and to monitor the locations of plastic deformation in the connections. Similarly, the FE analysis failure modes were identified by studying the shear versus displacement curve, shear versus principal strain in the shear tab, and by monitoring the stresses and the plastic deformation in the shear tab, bolts, and structural members.

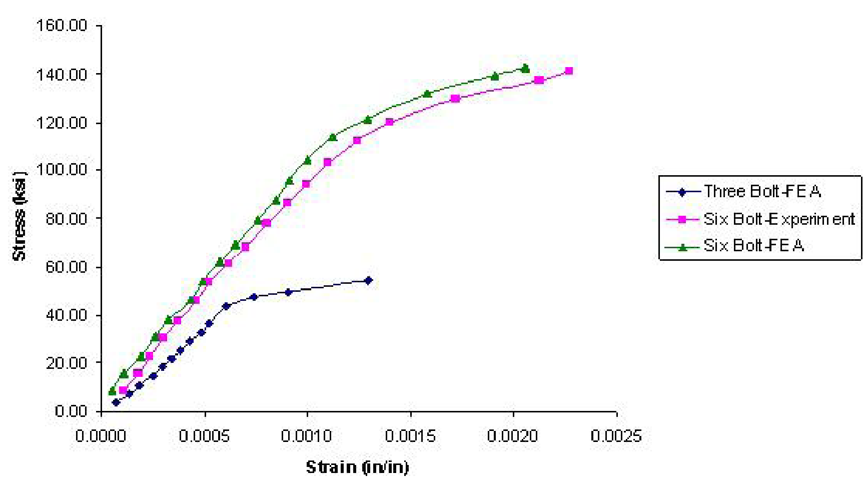

Fig. 11. Shear vs. principal strain.

The failure modes observed in both the experimental results and the FE analysis are bolt shear, bearing at the bolt holes, shear yield of the shear tab, web mechanism in the girder web, and twist in the shear tab. Three-bolt, six-bolt, 10-bolt, and 12-bolt connections, which are beam-to-girder connections, failed in bolt shear, bolt bearing, web mechanism, and twist in the shear tab. The bolt shear failure mode was identified in these connections by monitoring the stresses that developed in the bolts. In all these connections, the stresses in the bolts exceeded the yield strength of the bolt, which is 90 ksi, as shown in Figure 6. A typical bolt shear failure is shown in Figure 13; the stresses in the bolts reached 116 ksi, which is beyond the ultimate shear strength of the bolt (70 ksi).

The bolt holes in these connections also experienced high stresses and plastic deformation, as shown in Figure 16, and were in agreement with the experimental results, as shown in Figure 17, which identify the bolt bearing failure mode as a failure mode for these connections. In Figure 14, the stresses in the bolt holes reach 79 ksi, where the yield strength and

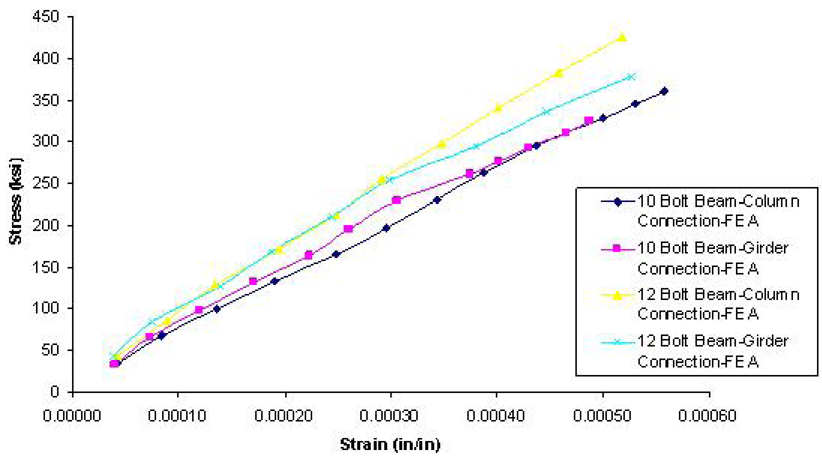

Fig. 12. Shear vs. principal strain.

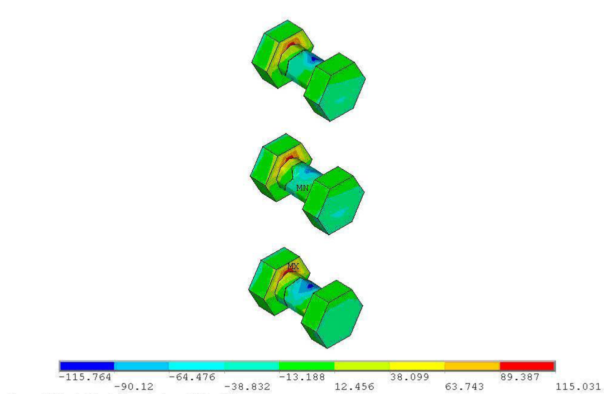

Fig. 13. Shear failure mode for the six-bolt connection model.

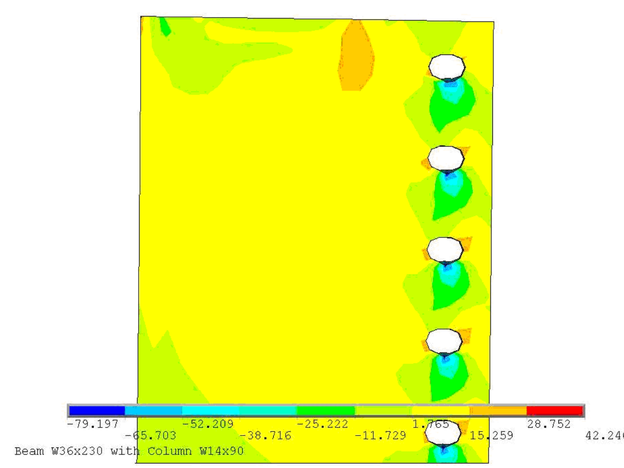

Fig. 14. Bolt bearing for the 10-bolt beam-to-column connection.

the ultimate strength are 49.6 ksi and 79 ksi, respectively, as defined in the material stress-strain response curves. Bolt bearing failure mode and the stresses in the vertical direction are also shown in Figure 18 for the 12-bolt beam-to-girder connection. Stresses in the shear tab about the *z*-axis for the 10-bolt beam-to-column connection are shown in Figure 19.

In the experimental work by Sherman and Ghorbanpoor, a rosette strain gauge was mounted on the shear tab to study the behavior of the connection plate. In the FE analysis, readings of the strain gauges were taken at the same location and compared to the experimental results for the six-bolt connection. The FEA results for the three-, 10-, and 12-bolt connection are reported in this paper to study the behavior of the connection plate. It is observed in Figure 11, for the three-bolt and the six-bolt connections that the shear tab has yielded at the location of the rosette, which identifies shear yield as a failure mode for these connections.

Web Mechanism in the Girder Web

Distortion in the web of the supporting girder was observed in the experiments for the three-bolt and the six-bolt connection. The stresses and the plastic deformations were monitored in the FE analysis for these connections and for the

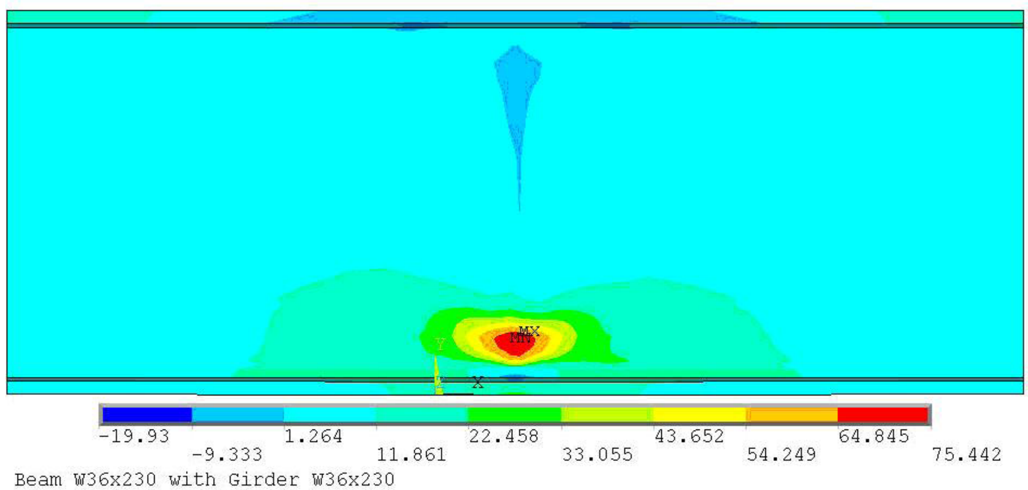

Fig. 15. Web mechanism failure mode in the girder's web for the 10-bolt beam-to-girder connection.

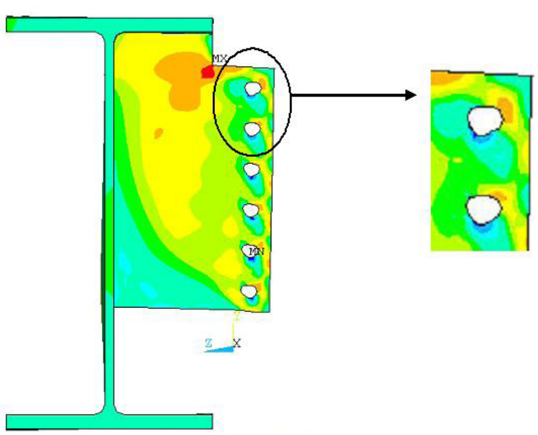

Fig. 16. Bolt bearing failure mode for the six-bolt beam-to-girder connection model.

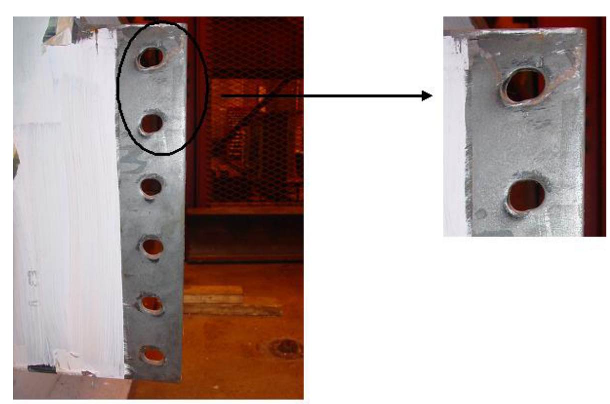

Fig. 17. Bolt bearing failure mode for the six-bolt beam-to-girder connection experiment.

10- and 12-bolt beam-to-girder connections. It was observed from the FE analysis that the web of the girders experience high stresses as shown in Figure 15, which identifies the web mechanism as a failure mode for the three-, six-, 10-, and 12-bolt beam-to-girder connections. It is observed from Figure 15 that the stresses at the tip of the shear tab reached 75 ksi where the yield strength and the ultimate strength of the shear tab are 61 and 75 ksi, respectively. Figures 20 and 21 show deterioration in the web of the girder for the six-bolt connections. The figures also show good agreement between the experimental and the FE analysis results.

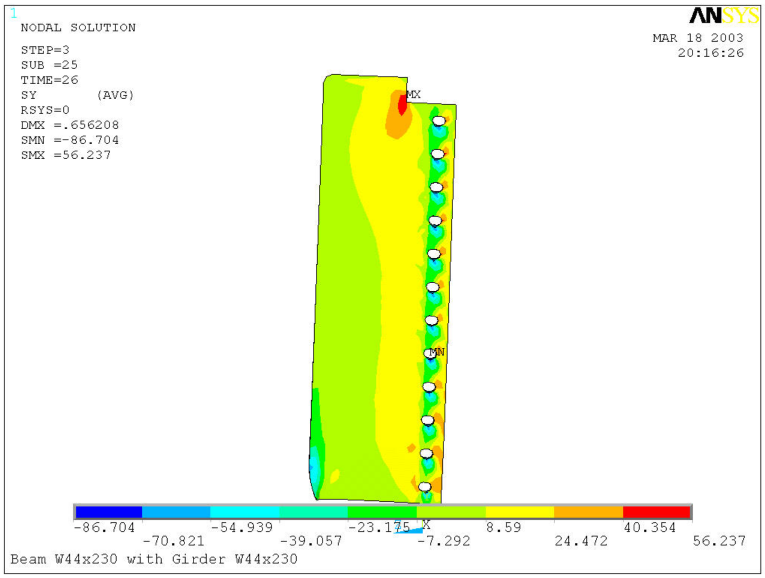

Fig. 18. Bolt bearing failure mode for the 12-bolt beam-to-girder connection.

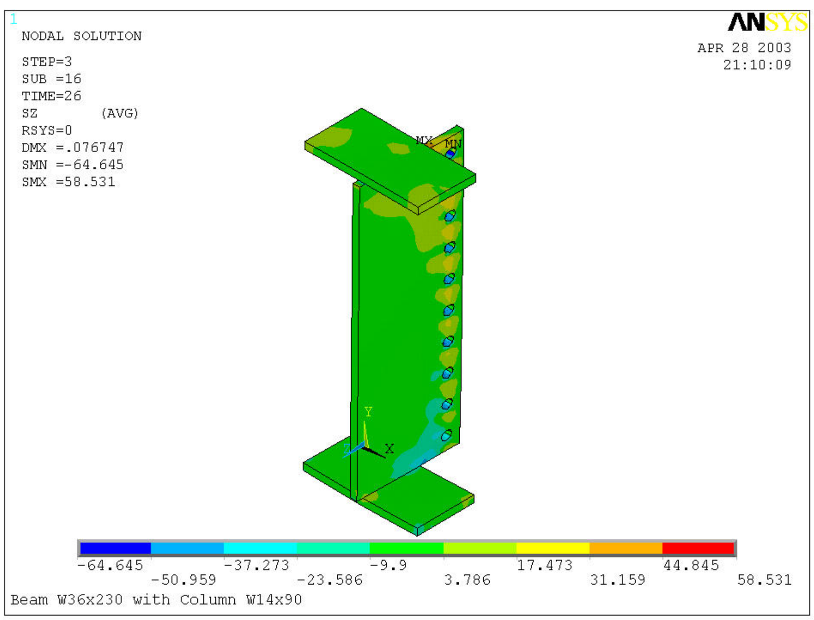

Fig. 19. Stresses in the shear tab about the z-axis in the 10-bolt beam-to-column connection.

Twist of the Shear Tab

As mentioned earlier, twist in the shear tab was more significant in the unstiffened shear tab connections. However, the stiffened connections experience twist in the beam-to-girder connections at the bottom of the shear tab. This was observed more in the shear tabs in deep connections, which identify twist as a secondary failure mode for these connections.

CONCLUSIONS

In this paper, the stiffened shear tab connections are evaluated in the elastic and plastic ranges up to failure analysis. This is Part II of a two-part article that addresses the unstiffened shear tab connections (Rahman et al., 2007). The experimental investigation (Sherman and Ghorbanpoor, 2002) showed severe vulnerability of unstiffened shear connections to twisting failure and low load-carrying capacity. The use of a stiffened shear tab connection is a viable design detail for shear tab steel construction. The paper investigates the behavior of such a connection by building 3D finite element models and performing the analyses in the linear and nonlinear ranges. The results of the FEA are compared with the experimental results performed on identical connections.

The results obtained from the FEA for the shear-deflection curves of the beam are within 16% deviation compared to the experimental results for the model three-bolt connection with a maximum deviation of 22%, and within 10% deviation for the six-bolt connection, and within 15% deviation for the eight-bolt connection. An even stronger correlation is observed when comparing the results of the principal strains for the six-bolt connection. The computation of eccentricity by the FE model shows a good agreement at ultimate load with a maximum percentile deviation of 12% for all connections.

The failure modes predicted by the FEA showed remarkable agreement with the failure modes of the connection during the experimental investigation. The location of high plastic strains, the bearing failure of the bolt holes, the web deterioration, and the twisting mechanism occurred in identical locations in the FE models as in the experiments. Such a model is a powerful tool in examining computed structural behavior. It represents the opportunity for the analyst and the designer to investigate full field results output for all the structural members. Following the same modeling and analysis procedures, the capacities and the failure modes of deep connections are obtained.

Based on the finite element and the experimental studies, unstiffened extended shear tab connections exhibit significant amount of twist that reduces the overall capacity of the connection. Twist failure mode was a primary failure mode for the five-bolt unstiffened connection. Therefore, unstiffened extended shear tab connections are not recommended.

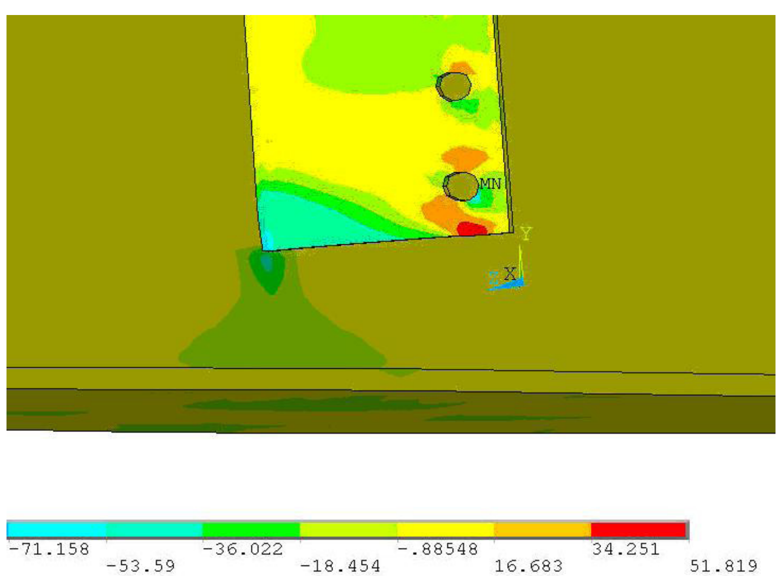

Fig. 20. Web mechanism failure mode for the six-bolt beam-to-girder connection model.

A yield line mechanism in the webs of the supporting columns and girders has been observed. This mechanism was observed in the columns and the girders of the unstiffened connections in the experimental study by Sherman and Ghorbanpoor (2002). The finite element analyses presented here confirm these findings.

Fig. 21. Web mechanism failure mode in the six-bolt beam-to-girder connection experiment.

REFERENCES

AISC (1995), *LRFD Manual of Steel Construction*, Volume II, 2nd ed., American Institute of Steel Construction, Inc., Chicago, IL.

AISC (1998), *LRFD Manual of Steel Construction*, Volume I, 2nd ed., American Institute of Steel Construction, Inc., Chicago, IL.

ANSYS (2002), User Manual, Theory Manual, Training Manual, Version 7.0, ANSYS, Inc., SAS IP, Inc.

Astaneh, A., Call, S.M., and McMullin, K.M. (1989), "Design of Single Plate Shear Connections," *Engineering Journal*, AISC, Vol. 26, No. 1, pp. 21–32, Chicago, IL.

Bursi, O.S. and Jaspart J.P. (1994), "Basic Issues in the Finite Element Simulation of Extended End-Plate Connection," *Computers and Structures*, Vol. 69, pp. 361–382.

Bursi, O.S. and Jaspart, J.P. (1997), "Benchmarks for Finite Element Modeling of Bolted Steel Connections," *Journal of Constructional Steel Research*, Vol. 43, No. 1, pp. 17–42.

Butterworth, J. (2003), "Finite Element Analysis of Structural Steelwork Beam-to-Column-Bolted Connections," *Constructional Research Unit*, School of Science and Technology, University of Teesside, UK, CS502-Issue 1, September 25.

Chiew, S.-P., Lie, S.-T., and Dai, C.-W. (2001), "Moment Resistance of Steel I-Beam to CFT Column Connections," *Journal of Structural Engineering*, ASCE, Vol. 127, No. 10, pp. 1164–1172.

Gebbeken N., Rothert, H., and Binder, B. (1994), "On the Numerical Analysis of End Plate Connections," *Journal of Constructional Steel Research*, Vol. 30, pp. 177–196.

Richard, R.M., Gillett, P.E., Kriegh, J.D., and Lewis, B.A. (1980), "The Analysis and Design of Single-Plate Framing Connections," *Engineering Journal*, AISC, Vol. 17, No. 2, pp. 38–52.

Rahman, A., Mahamid, M., Amro, A., and Ghorbanpoor, A. (2007), "The Analyses of Extended Shear Tab Steel Connections, Part I: The Unstiffened Connections," *Engineering Journal*, AISC, Vol. 44, No. 2, pp. 117–132.

Sherbourne, A.N. and Bahaari, M.R. (1994), "3D Simulation of End-Plate Bolted Connections," *Journal of Structural Engineering*, ASCE, Vol. 120, No. 11, pp. 3122–3136.

Sherbourne, A.N. and Bahaari, M.R. (1996), "3D Simulation of Bolted Connections to Unstiffened Columns-I T-Stub Connections," *Journal of Constructional Steel Research*, Vol. 40, No. 3, pp. 169–187.

Sherman, D. and Ghorbanpoor, A. (2002), "Design of Extended Shear Tabs," *Research Report RR3095*, American Institute of Steel Construction, Inc., Chicago, IL.

Yang, J.G., Murray, T.M., and Plaut, R.H. (2000), "Three-Dimensional Finite Element Analysis of Double-Angle Connections Under Tension and Shear," *Journal of Constructional Steel Research*, Vol. 54, pp. 227–244.